



A passive solar application using thermal energy storage in phase change materials for frost damage protection of citrus trees

Yalçın Yalaki¹ · Halime Ömür Paksoy²

Received: 20 February 2023 / Accepted: 27 August 2023 / Published online: 6 October 2023
© Akadémiai Kiadó, Budapest, Hungary 2023

Abstract

Increasing frequency of extreme weather conditions due to global climate change is threatening citrus orchards. Young seedlings and some citrus varieties like lemons are especially susceptible to frost damage. Many orchards have installed expensive wind machines that use electricity to ward off cold air. When the temperature falls below $-4\text{ }^{\circ}\text{C}$, even for several hours in a year, frost damage can kill citrus trees, thus causing serious economic losses. In this experimental study, we developed new phase change material (PCM) packages for passive solar protection of citrus trees from frost damage. Aqueous solutions of ethanol, ethylene glycol, and propylene glycol were evaluated as three PCMs due to their suitable chemical properties and abundance. Flexible packaging for the PCMs that can be easily applied to citrus trees were developed, and thermal protection performance of developed packages were tested on citrus seedlings. Supercooling of PCMs was seen as a problem during the tests, which was solved by adding a nucleating agent based on silver iodide developed in our laboratory. Results show that the ethanol containing PCM provided the longest thermal protection and succeeded in keeping seedling temperatures within the target interval for 10.5 h, while ethylene glycol and propylene glycol containing PCM packages provided 6.9 and 6.0 h of protection, respectively.

Keywords Phase change materials · Citrus trees · Frost damage · Thermal protection · Thermal energy storage

Introduction

Citrus are among the most produced and traded fruit crops around the world. Citrus orchards grow best in warm climates with temperatures ranging from 10 to 35 $^{\circ}\text{C}$. They are commonly grown in Mediterranean conditions [1]. Citrus trees are not tolerant to cold conditions or frost; young trees and flowered trees are especially susceptible to cold temperatures, while older trees are a bit more resistant. Photosynthetically active solar radiation plays a vital role in various stages of growth in citrus trees, and other factors such as temperature, soil moisture, and salinity should be at optimum levels for best utilization of solar energy in citrus orchards [2]. However, increase in extreme-temperature events because of global climate change often cause damage

to plants and decrease agricultural production [3, 4]. Frost is one of these events that may lead to fatal damages in plants. It occasionally occurs in the Mediterranean region, where citrus is an important agricultural product. Although the Mediterranean region generally has a mild climate, it is a known problem that the citrus plants are damaged during frost events in winter months [5]. Frost occurs when the air temperature falls below 0 $^{\circ}\text{C}$, especially at night [6]. Frost events are classified as mild, moderate, severe, and very severe based on damage to plants in general [7]. This classification is summarized in Table 1.

During frost events, most citrus plants begin to be damaged below $-4\text{ }^{\circ}\text{C}$ [8]. Frost damage affects the leaves, flowers, fruits, and trunks of citrus trees, but damage to trunk makes the recovery of the plant more difficult compared to the other parts [9]. In the literature, various methods are explained for protecting plants from frost damage. These methods involve some sort of thermal manipulation, and they include a wide variety of applications such as providing air circulation in cultivated areas, controlling the humidity of air and soil with irrigation, heating the cultivated areas with various heat sources, and spraying plants with various

✉ Yalçın Yalaki
yyalaki@hacettepe.edu.tr

¹ Faculty of Education, Hacettepe University, Ankara, Turkey

² Faculty of Arts and Sciences, Çukurova University, Adana, Turkey

Table 1 Classification of frost events based on plant damage [7]

Frost type	Temperature interval / °C and duration	Damage to the plant
Mild	0 to -2 (< 10 h)	Yellowing of foliage. Localized burns. Guide bud not affected
Moderate	-2.2 to 3.5 (10–20 h)	Foliage totally affected. Apical growth points damaged. Blackening of tissues
Severe	-3.5 to -6 (20–35 h)	Destruction of the foliage. Damage in apical growth point and stem portions (three internodes)
Very Severe	-3.5 to -6 (> 35 h)	Destruction of the foliage. Damage in apical growth point and in more than six buds and internodes

thermal preservatives [10–13]. A common method is to use expensive wind machines that relies on fossil fuels or electricity. Most of these methods are active systems that require additional energy to run pumps, fans, etc. In the only passive application found in the literature by Smyth and Skates [14], solar energy is utilized for protecting vineyards from frost. They designed a passive, solar-heated water filled quilt system in two vineyards and reported that the system increased the adjacent air temperature by up to 1 °C and decreased the duration of danger caused by frost.

Thermal energy storage (TES) for thermal protection of temperature-sensitive products through the use of phase change materials (PCM) is commonly used. TES systems can be classified into three categories based on storage method. These are sensible heat storage, latent heat storage, and thermo-chemical energy storage [15]. Among TES methods, latent heat storage has the advantage of higher-density energy storage within a limited volume. PCMs that change phase between solid and liquid states are the most commonly used latent heat storage mediums. PCMs with solid–liquid phase change do not cause large volume changes during charge and discharge cycles and operate at isothermal temperatures [16, 17]. There are various TES applications for sustainable use of renewables [18]; among them, PCMs offer unique solutions especially for thermal protection and regulation. These include storage of thermal energy in building materials [19], thermal regulation of electronic devices and batteries [20, 21], solar thermo-electric generator devices [22], textile applications for thermal comfort [23], and thermal protection of food during transport [24].

In this study, a novel passive frost protection method that utilizes solar heat for TES in PCMs was developed and tested [25]. The proposed method is potentially easier to use and cost-effective to protect citrus seedlings from frost damage at night compared to the expensive traditional methods that need fossil fuels or electricity. Although there are many studies in the literature about TES systems for thermal protection that use PCMs, we did not find any study about thermal protection of citrus plants from frost damage below -4 °C. The only application of PCMs for thermal regulation of plants that we could find was done by Beyhan et al. [26] for zucchini and pepper plants grown in a greenhouse by

hydroponic system without soil at around 10–15 °C. In this study, the authors' aim was to obtain optimum growing temperatures around the roots of plants. They developed a root-zone temperature control system based on TES in PCMs. Although they used PCMs to regulate root temperatures of plants, the study was not about protecting plants from frost damage at sub-zero conditions.

For sub-zero thermal protection applications, eutectic water-salt solutions are often used as PCMs [27–30]. These solutions are generally chemically unstable and corrosive, prone to supercooling (aka subcooling or undercooling) and phase segregation. In a recent study, binary mixtures of fatty acid methyl esters as phase change materials were investigated for such low-temperature applications [31]. Bio-based fatty acids as low-temperature PCMs may be very expensive and not easily available.

In this study, non-eutectic small molecule alcohol-water solutions were considered as alternative PCM candidates for sub-zero applications. Ethanol (E), ethylene glycol (EG), and propylene glycol (PG) have been investigated during PCM development. E is one of the most widely used alcohols in the industry, and EG and PG are frequently used as antifreeze in many applications, but they have not been used in frost protection of agricultural products. The advantages of these alcohols include non-corrosive property, ability to mix with water in all proportions (water-miscible), chemical stability, below 0 °C freezing points of their aqueous solutions, ability to control freezing point by adjusting concentration, and abundance. Three aqueous alcohol solutions with a new nucleating agent were developed as PCM candidates. The new PCMs were incorporated into flexible low-cost packaging which was also developed during this study. Results on PCM development and characterization, design of the PCM package, and thermal protection performances of the developed PCM packages are presented.

Material and methods

Materials

PCM operation temperature interval for thermal protection was chosen as -2 to -4 °C, considering that most citrus

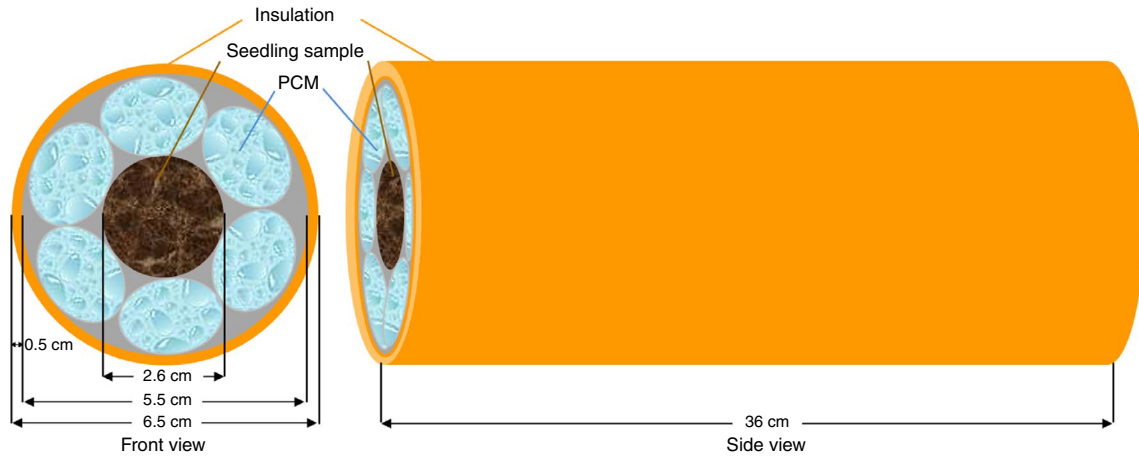


Fig. 1 Schematic view of the PCM package

plants begin to be damaged below $-4\text{ }^{\circ}\text{C}$. This temperature interval was chosen to achieve longer protection time by utilizing latent heat of phase change just before reaching hazardous temperature levels during a frost event. Various options were evaluated as packaging material for the prepared PCM solutions. A commercial product made from doped polyethylene (PE) with a lifetime of up to 36 months was chosen for its low cost, availability, and easy workability. Sheets of PE was processed with a plastic bonding machine and sample PCM packages were produced with

enough volume to fit 250 mL of PCM solution. Mastercare branded high-density polyethylene foam with a thickness of 5 mm and a density of 100 kg m^{-3} was chosen as an insulation material for the PCM packages. The insulation and PCM packages were wrapped around a citrus seedling sample and fixed with plastic clamps. The dimensions of each PCM package are shown schematically in Fig. 1. The total volume of the package was approximately 1195 cm^3 . The thickness of the insulation material and the PCM packages

Fig. 2 Change of ΔT_f with different concentrations of E, EG, and PG solutions [33]

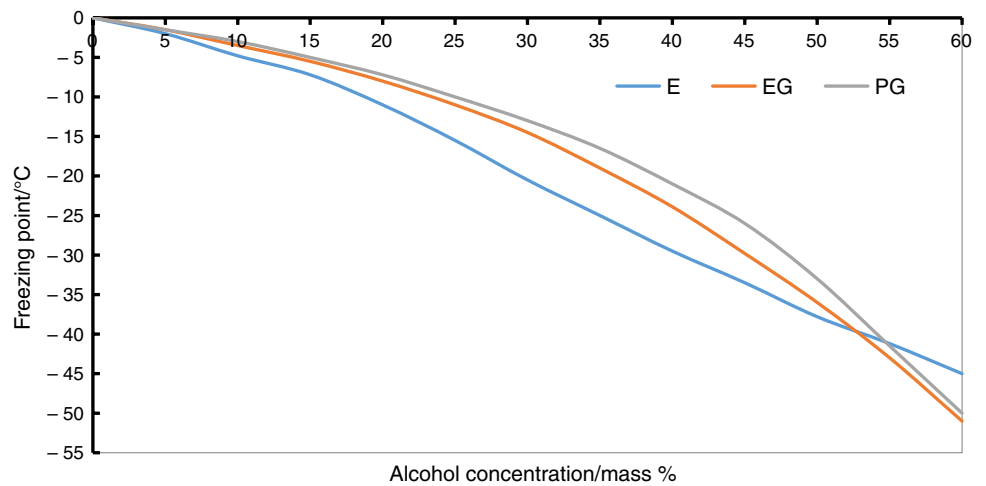


Table 2 Properties of the selected alcohols and their PCM solutions [34–38]

Alcohol	Pure alcohol molar mass (g/mol)	Pure alcohol freezing point /°C	g cm^{-3} (20/°C)	Freezing point of solution 10% v/v /°C	Concentrations in PCM solutions % v/v
E	46.07	-114	0.79	-4	6
EG	62.07	-13	1.11	-3.4	7
PG	76.09	-60	1.04	-3	10

Fig. 3 Programmed cooling–heating curve of the E-PCM, no phase change observed

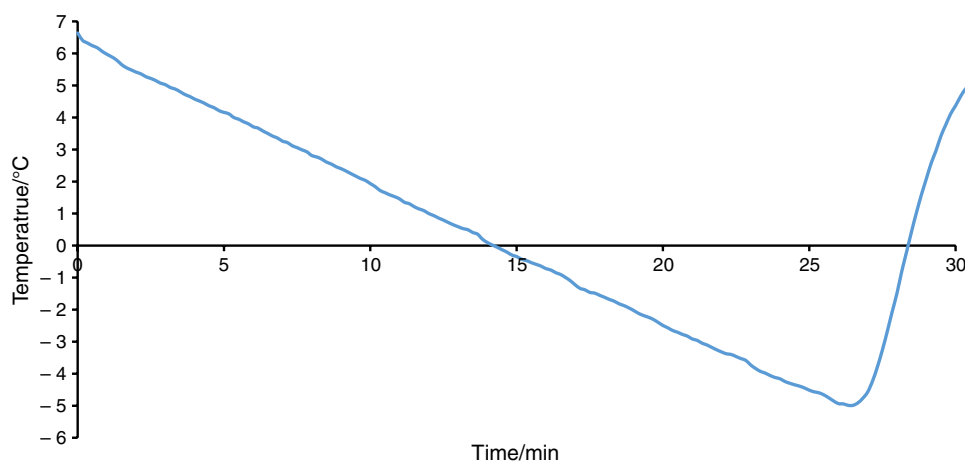
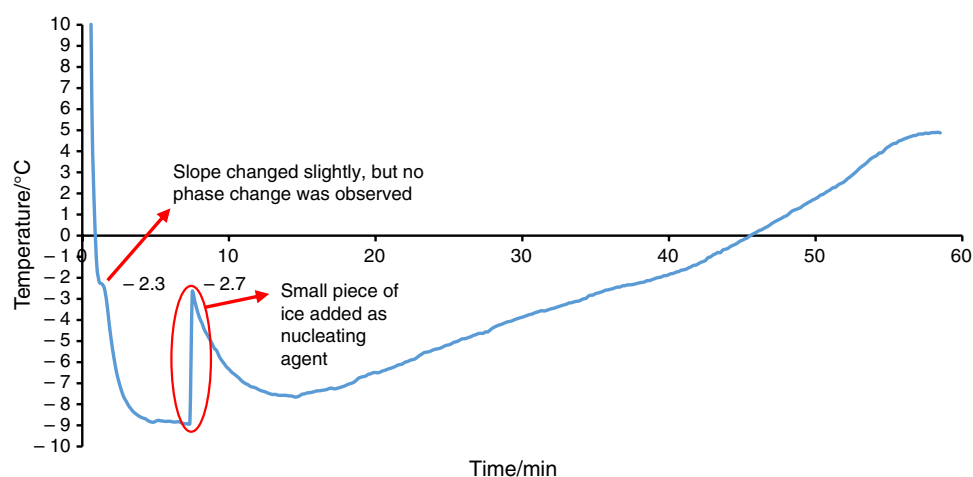


Fig. 4 Sudden cooling–heating curve of the E-PCM and the effect of adding ice as nucleating agent



around the seedling sample were 0.5 and 1.45 cm, respectively. This setup was used for experimental measurements.

Experiments

Melting and freezing performance of the prepared PCMs were determined with cooling–heating curves obtained by using thermostated water-EG mixture bath (Huber) and data logger (Agilent 34972A) instruments. T-type thermocouple sensors with accuracy of ± 0.5 °C was used for temperature measurements. Thermal conductivity of PCMs was measured with a thermal constants analyzer instrument (HotDisk 2500S model) with $1/10000$ W m⁻¹ K⁻¹ accuracy. Differential scanning calorimeter (DSC) measurements of PCM samples before and after thermal cycles were made with a DSC instrument (Mettler Toledo) with $1/100$ J g⁻¹ accuracy. To determine the thermal protection performance of PCMs, an incubator (Binder KB53 model) was used to setup a constant temperature environment. The interior of the incubator was adjusted to around -7 °C to simulate a frost condition. The developed

PCM packages were placed in this environment, and their thermal protection performances were examined using the data logger and thermocouple sensors. Post-freezing thaw times of PCM packages were compared with an infrared thermal camera (Testo 875-1i model). For these measurements, first three PCM packages containing E, EG, and PG were cooled down to -7.5 °C in the incubator, then they were allowed to warm at room temperature, while thermal images of the packages were taken at equal time intervals.

PCMs composed of mixtures may have problems such as separation of phases after melting–freezing cycles or a decrease in the performance of thermal regulation. Such problems are not expected with small molecule alcohol solutions; however, to determine the stability of prepared PCM solutions, DSC measurements before and after 100 thermal cycles were made. Thermal cycles were performed by placing three PCM solution samples simultaneously into a cold water-EG bath at -7.5 °C and subsequently into a warm water bath at 20 °C, and 100 cycles of freezing and melting were completed. Considering the frequency

Fig. 5 E, EG, and PG PCMs cooling–heating curves after addition of AgI as nucleating agent

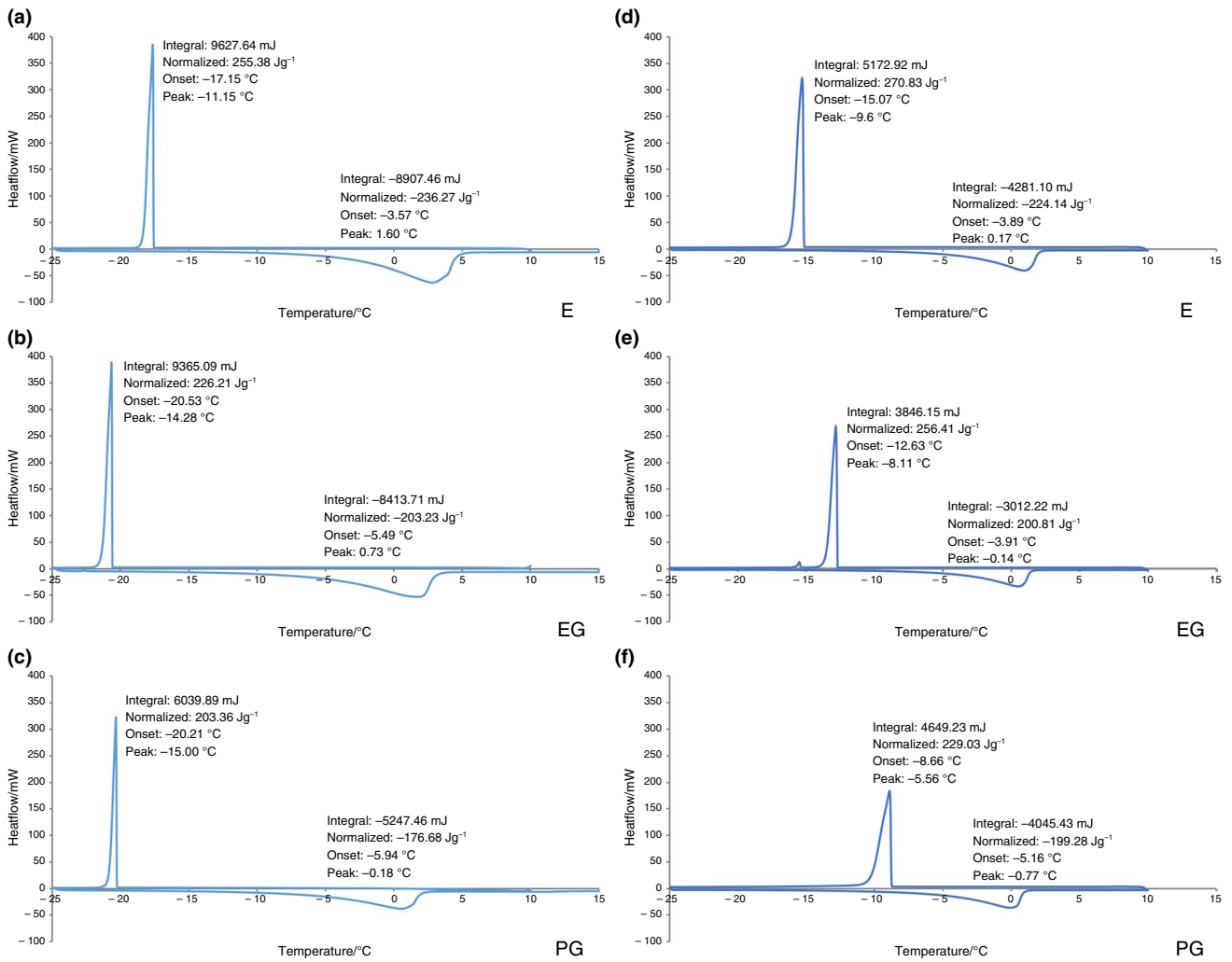
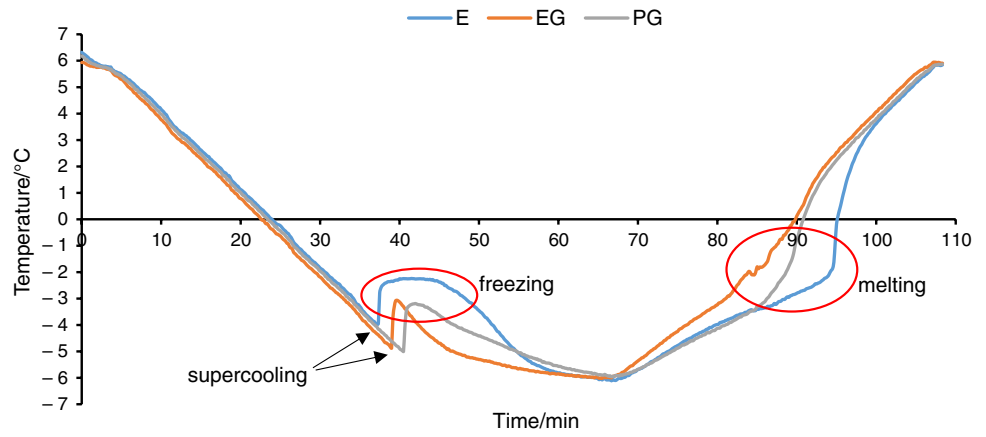


Fig. 6 Supercooling observed in DSC results of E, EG, and PG solutions before (a, b, c) and after 100 thermal cycles (d, e, f)

of frost in most Mediterranean regions, it was estimated that 100 thermal cycles represent approximately 10 years of use in ideal conditions. However, real lifetime of the PCM packages would probably be less due to many factors such as exposure to sunlight, high temperatures, and storage conditions.

Results and discussion

PCM development

For solar passive frost protection of citrus trees, PCMs that have freezing/melting temperature tailored for frost conditions are needed. The PCM should freeze during the night before reaching $-4\text{ }^{\circ}\text{C}$ and melt during the day with solar radiation without decomposition. This way solar energy is stored in PCM as sensible and latent heat. Aqueous alcohol solutions are prepared as PCM candidates to fit the given criteria. The concentrations of the aqueous alcohol solutions were determined based on freezing point depression equation $\Delta T_f = K_f \times m$ where K_f ($^{\circ}\text{C kg mol}^{-1}$) is the molal freezing point depression constant of water (which is 1.86) and m (mol/kg) is the molality of the solution [32]. Figure 2 shows the change of ΔT_f with different concentrations of alcohol solutions [33]. Based on this figure and data from the literature, three concentrations shown in Table 2 were chosen for candidate PCMs so that their phase change temperatures fall within the target temperature interval. As shown in Table 2, all three alcohol solutions prepared as PCMs are mostly water, and the alcohols have the role of adjusting the freezing temperature. It can be noted here that other concentrations of these alcohol solutions can be considered as PCMs for different temperature intervals for different applications.

Table 3 Thermal conductivity of PCM solutions

PCM solution /%v	Thermal Conductivity / $\text{W m}^{-1} \text{K}^{-1}$ 25 $^{\circ}\text{C}$
E (%6)	0.55
EG (%7)	0.43
PG (%10)	0.67

Cooling–heating curves

During the cooling–heating experiments, equal volumes of the PCM samples in test tubes were cooled in the water-EG bath. Figure 3 shows the cooling–heating curve of the E containing PCM (E-PCM) sample where the thermostated bath was programmed to cool to $-5\text{ }^{\circ}\text{C}$ in min. As shown in Fig. 3, no phase change was observed. In Fig. 4, the cooling–heating curve of the same PCM sample is shown, but this time, the sample was cooled from room temperature directly to $-9\text{ }^{\circ}\text{C}$ without a cooling program. Although a slight change of slope was measured at $2.3\text{ }^{\circ}\text{C}$, again no phase change was observed because of supercooling. To trigger phase change, a small piece of ice was added to the PCM at around 8th minute, and a sudden crystallization was observed, while the temperature raised to $-2.7\text{ }^{\circ}\text{C}$ from $-9\text{ }^{\circ}\text{C}$ as seen in the encircled region in Fig. 4.

The first cooling–heating curve experiments showed that supercooling was a problem for the selected PCMs. If not controlled, supercooling could prevent the use of latent heat in an application. Adding nucleating agents is one of the most common methods for overcoming the supercooling problem. Nucleating agents are substances that facilitate crystal formation in supercooled liquids or supersaturated solutions. Other methods include microencapsulation, use of nanofluid PCMs, and use of nanoparticles for nucleation [39]. For example, Mo et al. [40] described properties of nanofluid PCMs prepared by mixing TiO_2 nanoparticles with EG solutions. While nanoparticles acted as nucleating sites and enhanced the PCM by decreasing supercooling and increasing thermal conductivity, they also decreased the latent heat and storage capacity of the PCM.

Substances that have similar crystalline structure to the freezing substance can contribute to crystal formation and can be used as nucleating agents. It has been reported in the literature that the crystal structure of silver iodide (AgI) is similar to that of ice, and it is one of the best nucleating agents for water [41, 42]. Since PCMs developed in this study contain mostly water, AgI was a clear choice as a nucleating agent. AgI was synthesized in our laboratory by the precipitation reaction of silver nitrate (AgNO_3) and potassium iodide (KI) ($\text{AgNO}_{3(\text{aq})} + \text{KI}_{(\text{aq})} \rightarrow \text{AgI}_{(\text{s})} + \text{KNO}_{3(\text{aq})}$). In this synthesis, the aqueous solutions of AgNO_3 and KI were slowly mixed, and the precipitated AgI was filtered, washed, and dried. A small amount (less than 0.01% by mass) of the synthesized AgI was added to three PCMs, and cooling–heating curve experiments were repeated. Figure 5 shows the cooling–heating curves of the PCMs that included AgI as nucleating agent. In Fig. 5, it can be seen that supercooling still occurred but to a lesser degree. The

Fig. 7 Laboratory setup and application scheme: **a** seedling, thermocouple, PCM package, and insulation setup (red circles show locations of thermocouples), **b** placement of seedling-PCM package in the incubator, **c** schematic application of the PCM package on a citrus seedling

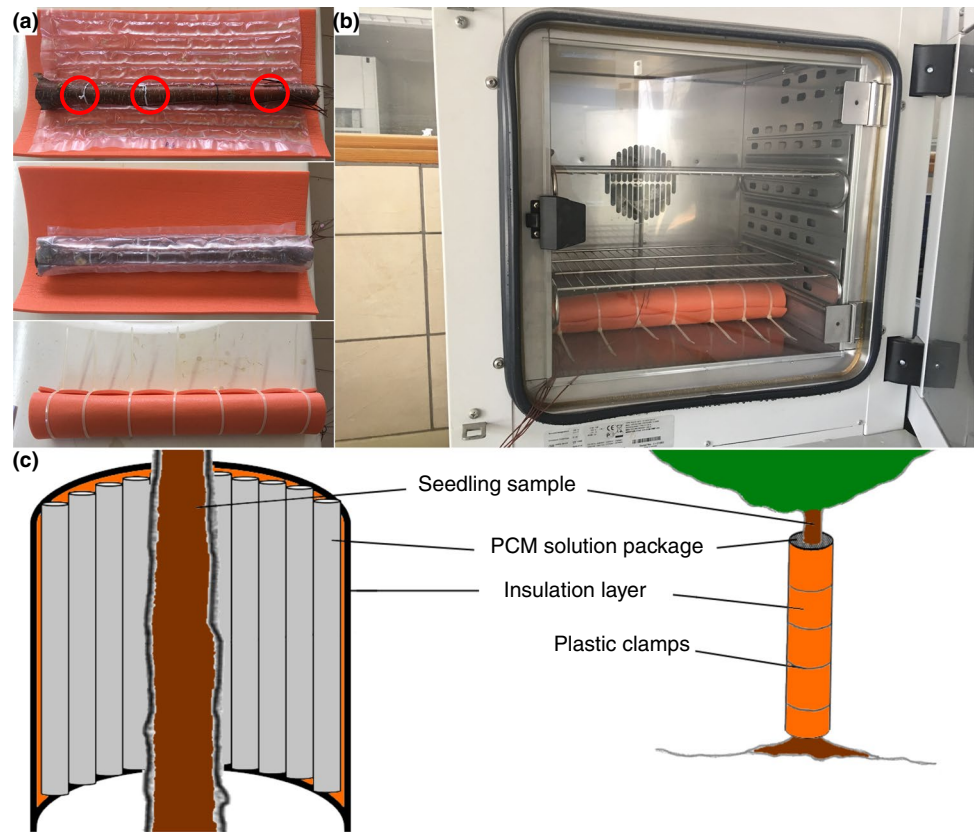
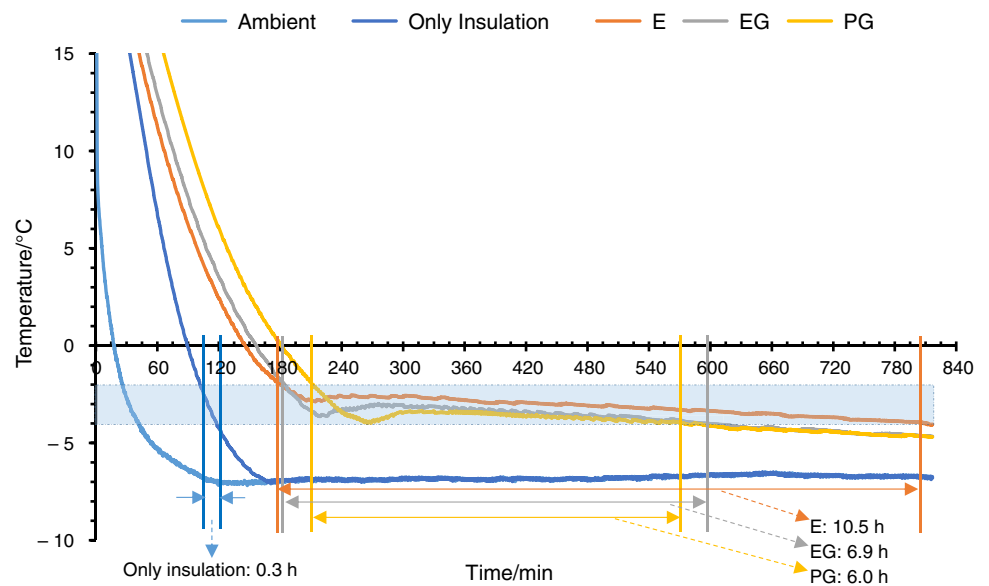


Fig. 8 Thermal protection performances of E, EG, and PG containing PCM packages



PCM containing E was supercooled down to -4°C , while the EG and PG containing PCMs were supercooled down to -5°C . After supercooling, freezing occurred very fast and their temperatures rose up to -2.2°C , -3.1°C and -3.2°C ,

respectively. These measurements showed that the freezing points of the PCM samples were in the target temperature interval. The phase change regions of the PCMs are encircled in Fig. 5. The E containing PCM's temperature rose

Table 4 Thermal protection duration of PCM packages and only-insulation

PCM Package	Thermal protection duration (hour) between -2 and -4 °C
E _(aq) + insulation	10.5
EG _(aq) + insulation	6.9
PG _(aq) + insulation	6.0
Only insulation	0.3

higher during freezing, and it kept the temperature at freezing point longer compared to the other two PCM candidates.

DSC results

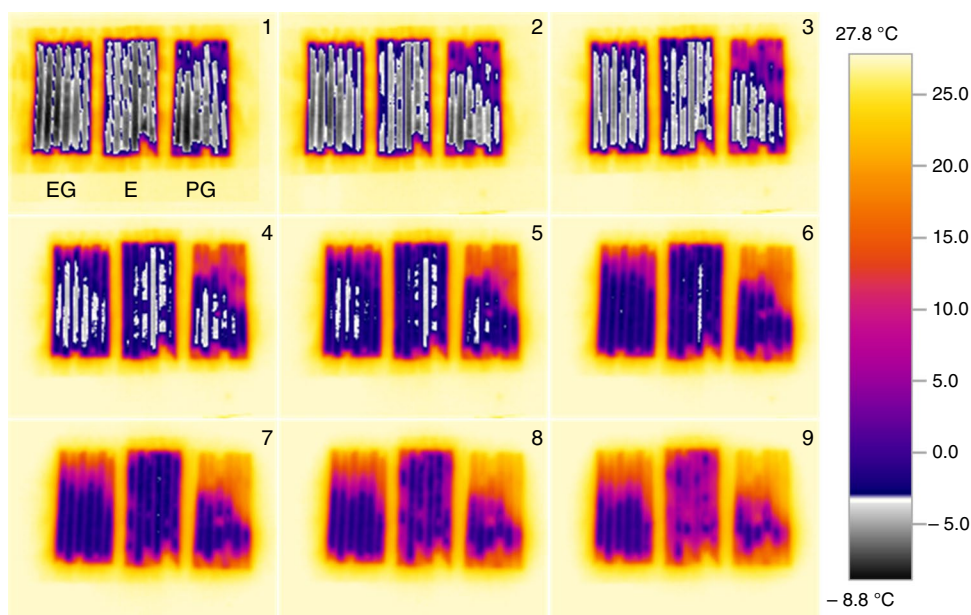
The problem of supercooling was also observed in DSC measurements as can be seen in the DSC curves of the prepared PCM solutions shown in Fig. 6 a, b and c. Melting and freezing peaks occurred well below expected temperatures as a result of supercooling. In DSC measurements that use mg of samples, the supercooling effects are commonly seen with materials of supercooling tendency. The freezing enthalpies of the E, EG, and PG containing PCMs were measured as 255 J g^{-1} , 226 J g^{-1} , and 203 J g^{-1} , respectively. Based on these results, it can be interpreted that E containing PCM gave more heat to the environment during freezing than others did; therefore, it is a better candidate to protect plants from frost damage. With regard to the melting enthalpies, the results for the E, EG, and PG were -236 J g^{-1} , -203 J g^{-1} , and 177 J g^{-1} , respectively. These results are in parallel with freezing enthalpies.

Thermal cycling results

The DSC measurements were repeated after 100 thermal cycles of freezing and melting, and no performance loss was observed in thermal cycles (Fig. 6 d, e and f). The freezing enthalpies of E, EG, and PG containing PCMs were measured as 271 J g^{-1} , 256 J g^{-1} , and 229 J g^{-1} , respectively. These values were slightly higher than the initial DSC measurements, but the order did not change. The enthalpy of the PCM containing E was again the highest. The melting enthalpies of the PCMs containing E, EG, and PG were measured as -224 J g^{-1} , -201 J g^{-1} , and -199 J g^{-1} , respectively. Similar to our findings, Sze et al. [43] reported that heat storage and recovery performances did not change and phase separation did not occur after thermal cycles of ethanol and ethylene glycol solutions used as PCMs at low temperatures.

Thermal conductivity results

In the literature, thermal conductivity of pure water has been reported as $0.6 \text{ W m}^{-1} \text{ K}^{-1}$ at 25 °C [44]. Since the PCM solutions used in this study were aqueous alcohol solutions containing mostly water, it was expected that their thermal conductivity would be close to that of water. Around 30 mL of each PCM solution was placed in a 50-mL beaker, and their thermal conductivities were measured at room temperature. Results of the thermal conductivity measurements are given in Table 3.

Fig. 9 False color thermal images of EG, E, and PG PCM packages taken at equal time intervals

Thermal protection performance of PCM packages

Each PCM package was wrapped around a citrus seedling stem sample, and temperature change was measured at 10 s intervals with three thermocouple sensors placed on the seedling sample to determine thermal protection performances. The seedling-PCM package setup was placed in the incubator, and the interior temperature was set to $-7\text{ }^{\circ}\text{C}$ to simulate a frost condition. The measurements were repeated with each of the PCM packages. A seedling-insulation setup without a PCM package was used for comparison. The laboratory setup for the experiments and schematic application of the PCM package on a seedling is shown in Fig. 7.

Thermal protection performances of PCM packages (plus insulation) and only-insulation package were measured. The insulation material used for all the experiments were the same with the same thickness (0.5 cm). Measurement results are given in Fig. 8, which shows that three PCM packages provided various durations of thermal protection, while only-insulation package provided little protection. The temperature values in Fig. 8 are average values of three thermocouples on the seedling sample, while ambient temperature was measured by one thermocouple. The PCM package containing E provided protection at around $-2.6\text{ }^{\circ}\text{C}$, and PCM packages containing EG and PG solutions provided protection at around $-3\text{ }^{\circ}\text{C}$ and $-3.5\text{ }^{\circ}\text{C}$, respectively, by releasing latent heat at these temperatures. All of the PCM packages kept the seedling temperature at the target interval of -2 and $-4\text{ }^{\circ}\text{C}$, which is shown with the blue rectangle region in Fig. 8 and prevented the temperature falling to critical levels. Figure 8 shows that the PCM package containing E provided protection for 10.5 h, the PCM packages containing EG and PG provided protection for 6.9 and 6.0 h, respectively, while insulation-only package provided 0.3 h of protection (Table 4). The protection durations, shown with arrows on Fig. 8, are determined between the points where temperature profile enters and leaves the blue rectangle region. These results are in agreement with the results from the cooling–heating curve and DSC measurements, which support that PCM package containing E had the longest thermal protection performance.

Thermal images

PCM packages containing E, EG, and PG were cooled down to $-7.5\text{ }^{\circ}\text{C}$ in the incubator, then they were left to thaw at room temperature and infrared images were taken with a thermal camera. Nine infrared images taken at 4.5 min intervals are given in Fig. 9. As indicated in the first image, the PCM package on the left contains the EG, the one in the middle contains the E, and the one on the right contains the

PG solutions. These images show that rate of temperature increase in PCM package containing E was slower than the others, which also showed that its melting time was longer. Together with the DSC and cooling–heating curve data, this observation suggests that the thermal energy storage capacity of the E containing PCM is higher, its temperature remains at freezing point longer, and the melting time is longer. These findings support that the E containing PCM has better potential for thermal protection among the three PCM candidates.

Conclusions

Three PCM packages were developed in this study as a novel method for frost protection that utilizes passive solar energy through thermal energy storage. Thermal performance of the developed PCMs with E, EG, and PG solutions was measured. The concentrations of the alcohol solutions were adjusted to change phase in the target temperature range of $-2\text{ }^{\circ}\text{C}$ to $-4\text{ }^{\circ}\text{C}$, which was determined based on classification of frost events reported in the previous studies. Only-water can also be used as PCM, and it would provide thermal protection at phase change temperature of water, around $0\text{ }^{\circ}\text{C}$ for appropriate applications. In this study, our aim was to have phase change happening as late as possible during a frost event at night (around $-2\text{ }^{\circ}\text{C}$ to $-4\text{ }^{\circ}\text{C}$ rather than $0\text{ }^{\circ}\text{C}$) to provide protection just before dangerous frost temperature levels. The PCM packages containing the E solution had better thermal protection performance. Temperature of the seedling sample used in the study was kept between -2 and $-4\text{ }^{\circ}\text{C}$ for 10.5 h with the E containing PCM package, while the EG and PG containing PCM packages provided 6.9 and 6.0 h of protection, respectively. We did not measure consecutive thermal protection performance of PCM packages, which is a limitation of this study. The PE sheets used in the preparation of the PCM packages were low cost and durable; however, alternatives with less environmental impact may be explored. Alternative insulation materials may also be investigated for better thermal protection. AgI was added as nucleating agent to all PCM packages to prevent supercooling. AgI is a good nucleating agent for water; however, it is listed with code H410 in GHS hazard statement [45] which means “very toxic to aquatic life with long lasting effects.” Therefore, the usage of AgI should be restricted to investigations in the laboratory, and it should be disposed according to regulations regarding the disposal of dangerous substances. AgI was only used to show the principle effect of a nucleating agent in this study, and more environmentally friendly alternatives should be explored to solve the nucleation problem. Further studies

are recommended to test the performance of the PCM packages under real conditions with alternative materials.

Author contribution YY involved in data curation, experimentation, visualization, investigation, and writing—original draft preparation, and HÖ.P involved in conceptualization, methodology, supervision, and writing—reviewing and editing.

Declarations

Conflict of interest The authors did not receive support from any organization for the submitted work. The authors declare that they have no known competing financial interests or personal relationships that could have appeared to influence the work reported in this paper.

References

- Abobatta WF. Managing citrus orchards under climate change. *MOJ Eco Environ Sci*. 2021. <https://doi.org/10.15406/mojes.2021.06.00212>.
- Sari M, Sonmez NK, Kurklu A. Determination of seasonal variations in solar energy utilization by the leaves of Washington navel orange trees (*Citrus sinensis* L. Osbeck). *Int J Remote Sens*. 2005. <https://doi.org/10.1080/01431160500104137>.
- Hatfield JL, Prueger JH. Temperature extremes: effect on plant growth and development. *Weather Clim Extremes*. 2015. <https://doi.org/10.1016/j.wace.2015.08.001>.
- Ma Q, Huang J, Hanninen H, Berninger F. Divergent trends in the risk of spring frost damage to trees in Europe with recent warming. *Glob Change Biol*. 2019. <https://doi.org/10.1111/gcb.14479>.
- Robinson C, Mort N. A neural network system for the protection of citrus crops from frost damage. *Comput Electron Agr*. 1997. [https://doi.org/10.1016/S0168-1699\(96\)00037-3](https://doi.org/10.1016/S0168-1699(96)00037-3).
- Asar M, Yalçın S, Nadaroplu Y, Erciyas H. Zirai Meteoroloji, TC. Çevre ve Orman Bakanlığı Devlet Meteoroloji İşleri Genel Müdürlüğü; <https://www.mgm.gov.tr/FILES/genel/kitaplar/zirai-meteoroloji.pdf>, 2008.
- Giardina J, et al. Frost severity effect on sprouting and seedling emergence of high quality seed cane in Tucuman Argentina. *Proc Int Soc Sugar Cane Technol*. 2013;28:1–11.
- Anderson JA, Gusta LV, Buchanan DW, Burke MJ. Freezing of Water in Citrus Leaves. *J Am Soc Hortic Sci*. 1983. <https://doi.org/10.21273/JASHS.108.3.397>.
- Zekri M, Oswalt C, Futch S, Hurner L. Freeze damage symptoms and recovery for citrus. *Citrus Industry*. 2016. <https://edis.ifas.ufl.edu/publication/HS1275> Accessed 10 Aug 2019.
- Martsof JD. Diversity of frost protection methodology. *Proc Fla State Hort Soc*. 2000;113:133–7.
- Perry KB. Basics of frost and freeze protection for horticultural crops. *Hort Tech*. 1998. <https://doi.org/10.21273/HORTTECH.8.1.10>.
- Turrell FM. The science and technology of frost protection. In: Reuther W, editor. *The Citrus Industry*, vol. 3. California: Univ. of Cal. Press; 1973. p. 338–446.
- Young FD. Frost and the Prevention of Frost Damage (No 1588). US Dept. of Agriculture, 1940.
- Smyth M, Skates H. A passive solar water heating system for vineyard frost protection. *Sol Energy*. 2009. <https://doi.org/10.1016/j.solener.2008.08.014>.
- Borri E, Sze JY, Tafone A, Romagnoli A, Li Y, Comodi G. Experimental and numerical characterization of sub-zero phase change materials for cold thermal energy storage. *Appl Energ*. 2020. <https://doi.org/10.1016/j.apenergy.2020.115131>.
- Pielichowska K, Pielichowski K. Phase change materials for thermal energy storage. *Prog Mater Sci*. 2014. <https://doi.org/10.1016/j.pmatsci.2014.03.005>.
- Nazir H, Batool M, Bolivar Osorio FJ, Isaza-Ruiz M, Xu X, Vignarooban K, et al. Recent developments in phase change materials for energy storage applications: a review. *Int J Heat Mass Tran*. 2019. <https://doi.org/10.1016/j.ijheatmasstransfer.2018.09.126>.
- Cabeza LF. *Advances in thermal energy storage systems: Methods and applications*. Cambridge: Woodhead Publishing; 2015.
- Malkawi DS, Tamimi AI. Comparison of phase change material for thermal analysis of a passive hydronic solar system. *J of Energy Storage*. 2021. <https://doi.org/10.1016/j.est.2020.102069>.
- Landini S, Waser R, Stamatiou A, Ravotti R, Worlitschek J, O'Donovan TS. Passive cooling of Li-Ion cells with direct-metal-laser-sintered aluminium heat exchangers filled with phase change materials. *Appl Therm Eng*. 2020. <https://doi.org/10.1016/j.applthermaleng.2020.115238>.
- Wei-Biao Y, Cong L, Si-Min H, Yuxiang H. Validation of thermal modeling of unsteady heat source generated in a rectangular lithium-ion power battery. *Heat Transf Res*. 2019. <https://doi.org/10.1615/HeatTransRes.2018026809>.
- Shittu S, Li G, Xuan Q, Xiao X, Zhao X, Ma X, Akhlaghi YG. Transient and non-uniform heat flux effect on solar thermoelectric generator with phase change material. *Appl Therm Eng*. 2020. <https://doi.org/10.1016/j.applthermaleng.2020.115206>.
- Su Y, Zhu W, Tian M, Wang Y, Zhang X, Li J. Intelligent bidirectional thermal regulation of phase change material incorporated in thermal protective clothing. *Appl Therm Eng*. 2020. <https://doi.org/10.1016/j.applthermaleng.2020.115340>.
- Singh S, Gaikwad KK, Lee YS. Phase change materials for advanced cooling packaging. *Environ Chem Lett*. 2018. <https://doi.org/10.1007/s10311-018-0726-7>.
- Yalaki Y, Paksoy HO. Protective That Include Phase Change Material for Thermal Protection of Citrus Trees. Patent registration number: 2019 18900, Turkish Patent and Trademark Office. 2020.
- Beyhan B, Paksoy HO, Dasgan Y. Root zone temperature control with thermal energy storage in phase change materials for soilless greenhouse applications. *Energy Convers Manage*. 2013. <https://doi.org/10.1016/j.enconman.2013.06.047>.
- Li G, Hwang Y, Radermacher R, Chun HH. Review of cold storage materials for subzero applications. *Energy*. 2013. <https://doi.org/10.1016/j.energy.2012.12.002>.
- Oró E, de Gracia A, Castell A, Farid MM, Cabeza LF. Review on phase change materials (PCMs) for cold thermal energy storage applications. *Appl Energ*. 2012. <https://doi.org/10.1016/j.apenergy.2012.03.058>.
- Safari A, Saidur R, Sulaiman FA, Xu Y, Dong J. A review on supercooling of phase change materials in thermal energy storage systems. *Renew Sustain Energy Rev*. 2017. <https://doi.org/10.1016/j.rser.2016.11.272>.
- Su W, Darkwa J, Kokogiannakis G. Review of solid–liquid phase change materials and their encapsulation technologies. *Renew Sustain Energy Rev*. 2015. <https://doi.org/10.1016/j.rser.2015.04.044>.
- Liston LC, Farnam Y, Krafcik M, Weiss J, Erk K, Tao BY. Binary mixtures of fatty acid methyl esters as phase change materials for low temperature applications. *Appl Therm Eng*. 2016. <https://doi.org/10.1016/j.applthermaleng.2015.11.007>.

32. Levine IA. Physical chemistry. 6th ed. New York: McGraw-Hill Higher Education; 2002.
33. Melinder Å . Thermophysical Properties of Aqueous Solutions Used as Secondary Working Fluids. Doctoral dissertation. Royal Institute of Technology. Sweden, 2007
34. Daubert TE, Danner RP. Physical and thermodynamic properties of pure chemicals, data compilation. Washington, DC: Taylor & Francis; 1987.
35. National Library of Medicine (NLM). 1,2-Ethanediol, CID=174. 2019. https://pubchem.ncbi.nlm.nih.gov/compound/1_2-Ethanediol. Accessed 10 Aug 2019.
36. National Library of Medicine (NLM). Ethanol, CID=702. 2019. <https://pubchem.ncbi.nlm.nih.gov/compound/Ethanol>. Accessed 10 Aug 2019.
37. National Library of Medicine (NLM). Propylene glycol, CID=1030. 2019. <https://pubchem.ncbi.nlm.nih.gov/compound/Propylene-glycol>. Accessed 10 Aug 2019.
38. Engineering ToolBox. Thermal conductivities for some common liquids. 2008. https://www.engineeringtoolbox.com/thermal-conductivity-liquids-d_1260.html. Accessed 15 Aug 2019.
39. Zahir MH, Mohamed SA, Saidur R, Al-Sulaiman FA. Supercooling of phase-change materials and the techniques used to mitigate the phenomenon. *Appl Energ*. 2019. <https://doi.org/10.1016/j.apenergy.2019.02.045>.
40. Mo S, Zhu K, Yin T, Chen Y, Cheng Z. Phase change characteristics of ethylene glycol solution-based nanofluids for subzero thermal energy storage. *Int J Energy Res*. 2017. <https://doi.org/10.1002/er.3599>.
41. Fukuta N. Experimental investigations on the ice-forming ability of various chemical substances. *J Meteorol*. 1958. [https://doi.org/10.1175/1520-0469\(1958\)015](https://doi.org/10.1175/1520-0469(1958)015).
42. Sano I, Fujitani Y, Maena Y. An experimental investigation on ice-nucleating properties of some chemical substances. *J Meteorol Soc Jpn Ser II*. 1956;34(2):104–10.
43. Sze JY, Mu C, Romagnoli A, Li Y. Non-eutectic phase change materials for cold thermal energy storage. *Energy Proc*. 2017. <https://doi.org/10.1016/j.egypro.2017.12.742>.
44. Engineering ToolBox. Water - thermal conductivity. 2018. https://www.engineeringtoolbox.com/water-liquid-gas-thermal-conductivity-temperature-pressure-d_2012.html. Accessed 15 Aug 2019.
45. LTS Research Laboratories Inc. Safety Data Sheet Silver Iodide. 2015. <https://www.ltschem.com/msds/AgI.pdf>. Accessed 29 Nov 2022.

Publisher's Note Springer Nature remains neutral with regard to jurisdictional claims in published maps and institutional affiliations.

Springer Nature or its licensor (e.g. a society or other partner) holds exclusive rights to this article under a publishing agreement with the author(s) or other rightsholder(s); author self-archiving of the accepted manuscript version of this article is solely governed by the terms of such publishing agreement and applicable law.